RESEARCH ARTICLE

Lamellipodia are crucial for haptotactic sensing and response

Samantha J. King[1,2], Sreeja B. Asokan[1,2], Elizabeth M. Haynes[1,2], Seth P. Zimmerman[1,3], Jeremy D. Rotty[1,2], James G. Alb, Jr[1,2], Alicia Tagliatela[1,2], Devon R. Blake[1,4], Irina P. Lebedeva[1,5], Daniel Marston[4], Heath E. Johnson[6], Maddy Parsons[7], Norman E. Sharpless[1,8], Brian Kuhlman[1,3], Jason M. Haugh[6] and James E. Bear[1,2,5,*]

ABSTRACT

Haptotaxis is the process by which cells respond to gradients of substrate-bound cues, such as extracellular matrix proteins (ECM); however, the cellular mechanism of this response remains poorly understood and has mainly been studied by comparing cell behavior on uniform ECMs with different concentrations of components. To study haptotaxis in response to gradients, we utilized microfluidic chambers to generate gradients of the ECM protein fibronectin, and imaged the cell migration response. Lamellipodia are fan-shaped protrusions that are common in migrating cells. Here, we define a new function for lamellipodia and the cellular mechanism required for haptotaxis – differential actin and lamellipodial protrusion dynamics lead to biased cell migration. Modest differences in lamellipodial dynamics occurring over time periods of seconds to minutes are summed over hours to produce differential whole cell movement towards higher concentrations of fibronectin. We identify a specific subset of lamellipodia regulators as being crucial for haptotaxis. Numerous studies have linked components of this pathway to cancer metastasis and, consistent with this, we find that expression of the oncogenic Rac1 P29S mutation abrogates haptotaxis. Finally, we show that haptotaxis also operates through this pathway in 3D environments.

KEY WORDS: Haptotaxis, Arp2/3, Lamellipodia, Directed migration

INTRODUCTION

Cell migration is crucial for many physiological processes (Ridley et al., 2003), often occurring *in vivo* in response to bound (haptotaxis), soluble (chemotaxis) or mechanical (durotaxis) cues. Haptotaxis is perhaps the least well-understood form of directional migration. It has long been known that cells can migrate up a gradient of adhered substrate (haptotaxis) *in vitro* (Carter, 1965), but the cellular and molecular mechanisms of this process are poorly understood. Haptotaxis is likely to contribute to many physiological and pathophysiological events, such as cutaneous wound healing (Sawicka et al., 2015; Clark, 1990), response to cardiovascular

[1]UNC Lineberger Comprehensive Cancer Center, The University of North Carolina at Chapel Hill, Chapel Hill, NC 27514, USA. [2]Department of Cell Biology and Physiology, The University of North Carolina at Chapel Hill, Chapel Hill, NC 27599, USA. [3]Department of Biochemistry and Biophysics, University of North Carolina, Chapel Hill, NC 27599, USA. [4]Department of Pharmacology, University of North Carolina at Chapel Hill, School of Medicine, Chapel Hill, NC 27599, USA. [5]Howard Hughes Medical Institute, The University of North Carolina at Chapel Hill, Chapel Hill, NC 27599, USA. [6]Department of Chemical & Biomolecular Engineering, North Carolina State University, Raleigh, NC 27695, USA. [7]King's College London, Randall Institute, London SE1 8RT, UK. [8]Department of Genetics, The University of North Carolina at Chapel Hill, Chapel Hill, NC 27599, USA.

*Author for correspondence (jbear@email.unc.edu)

J. E.B., 0000-0002-8489-996X

disease (Takawale et al., 2015), atherosclerosis and cancer progression (Kostourou and Papalazarou, 2014; Aznavoorian et al., 1990; Wolf and Friedl, 2011). Understanding the mechanism of haptotaxis will be crucial for dissecting the relative contributions of various directional migration cues during these events.

One prominent feature of migrating adherent cells is a leading-edge fan-shaped protrusion called the lamellipodium. Although these have been known for decades and widely studied, their precise function and absolute requirement for motility are controversial. Our lab has previously demonstrated that the Arp2/3 complex is required for the formation of lamellipodia in fibroblasts (Wu et al., 2012; Rotty et al., 2015). The Arp2/3 complex nucleates actin filaments from the sides of existing filaments to create branches (Pollard, 2007). Cells lacking the Arp2/3 complex are capable of chemotax along a gradient of PDGF, but cannot haptotax on gradients of various extracellular matrix proteins (ECMs), including fibronectin, laminin and vitronectin (Asokan et al., 2014; Wu et al., 2012). However, because Arp2/3-branched actin is utilized in a variety of cellular processes in addition to lamellipodia formation – including endocytosis and retromer-mediated sorting – the abrogation of haptotaxis that accompanies the loss of the Arp2/3 complex might involve any or all of these processes. Elucidating exactly how the Arp2/3 complex is utilized to facilitate haptotaxis will be crucial for our understanding of this process.

Small GTPases play key roles in linking plasma membrane signaling events to the dynamic regulation of the actin cytoskeleton, including activating nucleation-promoting factors (NPFs) that activate the Arp2/3 complex at various cellular locations (Campellone and Welch, 2010). For example, Rac1 localizes to the leading edge of cells and can regulate the lamellipodia through the WAVE regulatory complex (WRC). Rac1 relieves WRC auto-inhibition, allowing WAVE to activate the Arp2/3 complex (Chen et al., 2010; Kobayashi et al., 1998). As with most small GTPases, Rac1 cycles between GTP-bound active and GDP-bound inactive states. Interestingly, a rapid-cycling mutation of Rac1, P29S, has recently been identified as a putative driver mutation in melanoma and is associated with disease progression and metastasis (Halaban, 2015; Krauthammer et al., 2012; Mar et al., 2014). The cycling of small GTPases is regulated by guanine nucleotide exchange factors (GEFs), GTPase-activating proteins (GAPs) and GDP dissociation inhibitors (GDIs) (Lawson and Burridge, 2014). Of particular relevance for haptotaxis, a subset of GEFs for Rac1 are activated by ECM adhesion (Kutys and Yamada, 2014), including β-Pix (Rho guanine nucleotide exchange factor 7; ARHGEF7) and T-Cell lymphoma invasion and metastasis 1 (Tiam1) (Boissier and Huynh-Do, 2014; Wang et al., 2012).

Cells engage the ECM through a variety of surface receptors, with integrins being the most significant contributors (Hynes, 2002). During integrin activation, proteins cluster at their cytoplasmic tails, forming nascent adhesions. A subset of these adhesions becomes

mature through the recruitment of additional proteins to form focal complexes, and later mature into focal adhesions (Webb et al., 2002). Although focal adhesions and focal complexes contain similar sets of adhesion proteins, focal complexes are smaller and comprise more phosphorylated (activated) adhesion proteins. Focal adhesion kinase (FAK) and Src-family kinases (SFKs) are two key types of kinase operating at focal complexes and adhesions. FAK and SFKs play key roles in cell migration and invasion, as well as in a variety of other cellular processes. They are activated through phosphorylation of tyrosine residues, and their activated forms have higher levels of localization at focal complexes than at mature adhesions (Mitra and Schlaepfer, 2006).

In this study, we sought to understand the cellular basis of haptotaxis by systematically dissecting the specific pathway upstream of the Arp2/3 complex that is required. Although the molecular components required for cells to adhere to ECM and generate lamellipodia have been extensively studied, these have not been studied in the context of gradients of proteins in the ECM. We have elucidated a specific molecular pathway, in both two- and three-dimensional (2D and 3D, respectively) environments, whereby haptotaxis is controlled through differential lamellipodial dynamics.

RESULTS
Differential lamellipodial protrusion dynamics regulate haptotaxis

In order to dissect the mechanism of haptotaxis, we utilized microfluidic chambers to generate gradients of fluorescent fibronectin and directly observed cells during directional migration, as described previously (Wu et al., 2012; Chan et al., 2014). Two methods were developed to control for gradient differences between chambers. (1) Differential labelling – we used combinations of cell tracker dyes and fluorescent protein expression to differentiate between control cells and cells expressing small hairpin (sh)RNAs or alternative isoforms. These mixtures of cells were plated together on the same gradients to ensure faithful comparisons and control for potential non-autonomous effects. For all RNA interference (RNAi) experiments, two independent shRNAs were used. (2) A drug wash-in protocol – this allows for directed comparison of non-drug-treated versus drug-treated cells on the same gradients. After 7 h of observation, drug was added, and the same cells were tracked for at least another 7 h.

To quantify haptotaxis, we used single-cell tracking and visualized tracks as a rose plot (each segment shows the frequency of tracks in that direction) (Fig. 1A). We have used a forward migration index (FMI) to quantify haptotaxis throughout the paper. FMI is defined as the displacement of the cell in the direction of the gradient divided by the total distance migrated; typical values for fibroblast haptotaxis on fibronectin gradients fell in the range 0.15–0.25. An average FMI with 95% confidence intervals encompassing 0 was not considered significantly different from random migration (Fig. 1A). In addition, velocity (µm/h) and persistence (displacement divided by total track length, d/T) were calculated (Fig. 1A). If a cell failed to move, a defect in the general migration machinery could not be distinguished from a defect in directional sensing or response. Therefore, treatments that abrogated movement were not investigated.

Previously, we have shown the importance of the Arp2/3 complex for haptotaxis using RNAi-based depletion experiments (Wu et al., 2012). To confirm the role of the Arp2/3 complex in haptotaxis using a complete deletion approach, we used fibroblasts from conditional knockout $Arpc2^{-/-}$ mice [mouse tail fibroblasts

(MTFs)] along with their matched wild-type (WT; pre-Cre recombination) and rescue lines ($Arpc2^{-/-}$ MTFs re-expressing GFP-tagged Arpc2) (Fig. S1C, KOR) (Rotty et al., 2015). Loss of the $Arpc2$ gene, encoding the essential Arpc2 subunit of the Arp2/3 complex, depletes all subunits of the Arp2/3 complex, and re-expression of Arpc2 rescues the entire complex (Fig. S1C). WT MTFs are able to haptotax towards higher concentrations of fibronectin, whereas $Arpc2^{-/-}$ MTFs [knockout (KO)] cannot (Fig. 1B; Fig. S1L). Re-expression of Arpc2 [knockouts with rescue (KOR)] restores haptotaxis (Fig. 1B; Fig. S1L). $Arpc2^{-/-}$ MTFs migrated significantly more slowly than either of the WT or rescue counterparts; however, persistence was unaltered (Fig. S1D,L). To further confirm this result in a different cell type, we treated vascular smooth muscle cells (VSMC) with a small-molecule inhibitor of the Arp2/3 complex, CK666, and observed no haptotaxis (Fig. 1C; Fig. S1E,L). In addition, cytochalasin D (CytoD), at a concentration that slows actin polymerization without fully preventing it (100 nM), abrogated fibroblast haptotaxis (Fig. S1F–H,L). At this concentration, our previous work has shown that CytoD primarily affects Arp2/3-based actin structures (Rotty et al., 2015), further implicating dynamic branched actin in haptotaxis.

Because the Arp2/3 complex is crucial for haptotaxis, we hypothesized that the lamellipodial dynamics relative to the fibronectin gradient in haptotaxing cells would be different in cells moving up the gradient versus those moving up down the gradient. Kymography analysis of short-lived lamellipodial protrusions over four quadrants of the cell was performed on fibroblasts undergoing haptotaxis or random migration (Fig. 1D). Fibroblasts display differential lamellipodial dynamics during haptotaxis but, intriguingly, not during random migration (Fig. 1E; Fig. S1I,J). During haptotaxis, protrusions extending up the gradient (the area of the cell in contact with the highest concentration of fibronectin) lasted longer and advanced further than protrusions extending down the gradient (the area of the cell in contact with the lowest concentration of fibronectin) or to the sides (Fig. 1E), with no difference in the velocity of either protrusion or retraction (Fig. S1I). By contrast, during random migration, protrusions formed in any direction had similar protrusion and retraction dynamics (duration, distance and velocity) (Fig. S1J). Furthermore, when we examined lamellipodial dynamics at the same concentration of CytoD that abrogates haptotaxis, treated cells no longer displayed differential lamellipodial dynamics seen in untreated, haptotaxing cells (Fig. S1K).

We hypothesized that lamellipodia protruding up a haptotactic gradient (towards increasing concentration of fibronectin) would be more stable than lamellipodia protruding down the gradient. To directly test this hypothesis, we used a recently developed cellular optogenetic approach to locally activate Rac1 and trigger lamellipodial protrusion using light-induced membrane targeting of the Dbl homology and pleckstrin homology (DH-PH) domains of Tiam1 (Fig. 1Fi) (Guntas et al., 2015). Using this approach, we were able to simultaneously direct protrusions both up and down the fibronectin gradient in fibroblasts undergoing haptotaxis (Fig. 1Fii). When light is applied to a region in the cell, a protrusion is formed, and when the light is removed, the protrusion retracts, as quantified using kymography (Fig. 1Fii and Fiii). Interestingly, protrusions directed up the gradient formed faster and advanced further than protrusions directed down the gradient; however, there was no difference in the retraction of these protrusions (Fig. 1G). Taken together, these data suggest that differential lamellipodial dynamics are a crucial cellular mechanism of haptotaxis.
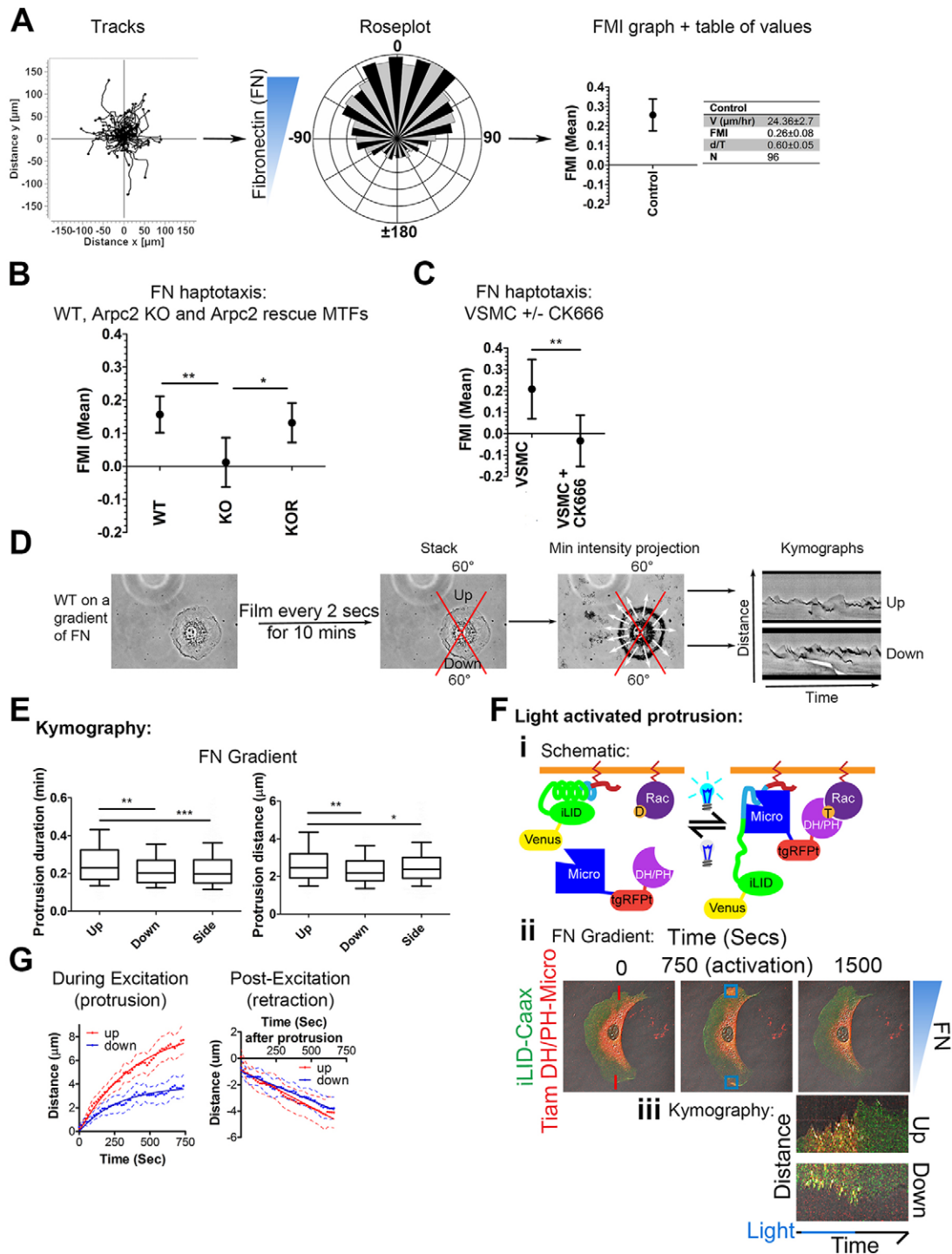
Fig. 1. Differential lamellipodial protrusion dynamics regulate haptotaxis on fibronectin. (A) Example of the flow of data from a 2D fibronectin (FN) haptotaxis experiment. After manual tracking of the cells, an example track plot is shown. The rose plot shown is generated from those tracks (the blue triangle shows the direction of the fibronectin gradient with respect to the segments). Forward migration index (FMI), defined as displacement in the gradient direction divided by total track length, was calculated from the track files. FMI is plotted graphically, showing the mean±95% confidence intervals (C.I.s). N=number of tracks, d/T=Persistence (displacement/total track length) and V=velocity (μm/h). (B) FMI graph (mean±95% C.I.s) for haptotaxis in response to fibronectin of WT, *Arpc2* KO and *Arpc2* KO+Arpc2–GFP (Arpc2 KO rescue, KOR) mouse tail fibroblasts (MTFs). (C) FMI graph (mean±95% C.I.s) for fibronectin haptotaxis of VSMCs with CK666 (150 μM) washed in. (D) Schematic example of how kymography analysis was performed, with example kymographs, up (60°) vs down (60°), relative to the gradient, for WT IA32 fibroblasts on a gradient of fibronectin. (E) Kymography analysis on a gradient. In the box-and-whisker plot, the box represents the 25–75th percentiles, and the median is indicated. The whiskers show the 10–90th percentiles. Four chambers, 26 cells. (Fi) Schematic for protrusion generation through activation with light. Terms are as defined in Guntas et al., 2015. (Fii) Example image for protrusion generation and retraction (light activation, then off) up and down the gradient for a fibroblast on a gradient of fibronectin (500 μg/ml at source). (Fiii) Example kymographs up versus down, from a single cell, from this experiment. (G) Graphs (mean±s.e.m.) from kymographs for the cell edge up (red) vs down (blue) under protrusion generation (light activation) or retraction (after light activation). Student's *t*-tests (to compare two data sets) or one-way ANOVA with Bonferroni's Multiple Comparison test (to compare more than two data sets), *P<0.05, **P<0.01 and ***P<0.001.

Differential actin dynamics regulated through Arp2/3 complex activity are essential for haptotaxis

Because CytoD, which disrupts actin dynamics, abrogates haptotaxis and the differential lamellipodial dynamics seen during haptotaxis, we hypothesized that the dynamics of actin within the lamellipodia are also differentially regulated to control haptotaxis. To investigate this possibility, fluorescence recovery after photobleaching (FRAP) was performed on fibroblasts expressing GFP-tagged actin during haptotaxis or movement on a uniform fibronectin concentration (Fig. S1M). Interestingly, actin at the cell edge up the gradient is more dynamic (recovers at a faster rate) than actin at the cell edge down the gradient, with no significant difference between the actin dynamics in cells on uniform fibronectin (Fig. 2A; Fig. S1N). Furthermore, this difference in actin dynamics was not observed on gradients of fibronectin when cells were treated with CK666 (Fig. 2B), indicating that the Arp2/3 complex is responsible for this difference in actin dynamics.

Because haptotaxis is regulated through differential actin and lamellipodial dynamics through Arp2/3 activity, we hypothesized that the Arp2/3 complex itself might be differentially localized during haptotaxis. In order to monitor molecular events within individual cells as they engaged in haptotactic or random migration, we developed a correlative immunofluorescence protocol. Live cells were observed haptotaxing or random migration on a uniform fibronectin concentration, followed by fixation and staining with specific antibodies (Fig. 2C). To analyze the resulting images, we used an unbiased program that calculates the amount of high-intensity staining at the cell edge, relative to the extrinsic gradient or direction of migration (Fig. 2C; Fig. S1O) (Johnson et al., 2015; Haynes et al., 2015). During haptotaxis, the Arp2/3 complex (visualized by staining the endogenous Arpc2 subunit) was more concentrated at the cell edge up the gradient than at the edges down the gradient or at the sides of the cell (Fig. 2D, left). However, during random migration, the Arp2/3 complex showed no significant difference in its localization at the cell edge relative to the direction of migration (Fig. 2D, right). In order to test whether this differential localization of Arp2/3 is sufficient to drive migration in a directed fashion, we inhibited the activation of the Arp2/3 complex differentially across cells using a gradient of CK666. Fibroblast migration on a gradient of CK666 was biased away from the source of CK666 (Fig. 2E; Fig. S1P,Q). Therefore, differences in the activation state of the Arp2/3 complex across a single cell are sufficient to drive directed migration.

The WRC is required for haptotaxis, whereas N-WASP and WASH are dispensable

The Arp2/3 complex is activated through NPFs that are required for different cellular processes: the WRC in lamellipodia formation, N-WASP in endocytosis and WASH in retromer-mediated sorting (Rotty et al., 2013). Because all of these cellular processes could plausibly be involved in haptotaxis, discovering which NPF(s) is required for haptotaxis would provide insight into the cellular mechanisms of haptotaxis. The WRC can utilize one of three isoforms of WAVE proteins: WAVE1, WAVE2 or WAVE3 (also known as WASF1, WASF2 and WASF 3, respectively). In order to deplete cells of all forms of the WRC, we depleted an obligate subunit of the complex (Nap1; also known as NCKAP1) as described previously (Tang et al., 2013). Upon depletion of Nap1, we observed the expected co-depletion of the different WRCs (hereafter collectively referred to as the WRC) without affecting the levels of the other NPFs, such as N-WASP (Fig. S2A). Depletion of the WRC through knockdown of *Nap1* abrogated haptotaxis

without affecting velocity or persistence (Fig. 3A; Fig. S2C,F,K). Interestingly, depletion of either N-WASP or WASH in fibroblasts (Fig. S2B) did not significantly affect haptotactic fidelity, migration velocity or persistence (Fig. 3B,C; Fig. S2D,E,G,H,K). These data indicate that the WRC, but not the other NPFs, is required for fibronectin haptotaxis. The lack of defects in haptotaxis with N-WASP and WASH depletion suggests that Arp2/3-regulated vesicular trafficking does not appear to play a major role in haptotaxis under these conditions. Because the WRC is involved in lamellipodia formation, this corroborates our previous data that regulation of lamellipodial protrusions is crucial for haptotaxis.

To determine if a particular WAVE isoform regulates haptotaxis, we depleted individual WAVE isoforms (Fig. S2B). Depletion of WAVE2 significantly decreased the ability of the cells to haptotax, whereas depletion of either WAVE1 or WAVE3 did not alter their haptotactic ability (Fig. 3D; Fig. S2I,L). To discern whether or not WAVE2 is differentially localized in haptotaxing fibroblasts, as seen with the Arp2/3 complex, we performed correlative immunofluorescence for WAVE2. Like the Arp2/3 complex, WAVE2 was also differentially localized in fibroblasts during haptotaxis, with enrichment at the cell edge that extended up the gradient relative to that in the down gradient portion or that at the sides of the cell (Fig. 3E,F, left). N-WASP was also localized at the leading edge, similar to WAVE2 and Arp2/3. However, N-WASP was not differentially localized during haptotaxis (Fig. 3E,F, right). Therefore, the differential localization seen for WAVE2 and Arp2/3 is not attributable to a general asymmetry of leading edge markers; rather, specific proteins required for haptotaxis are differentially recruited during haptotaxis.

Rac1 and the Rac GEF Tiam1 are essential for fibroblast haptotaxis through the WAVE–Arp2/3 pathway

Rac1 promotes lamellipodia formation through its ability to activate the WRC. Therefore, we postulated that Rac1 is central to haptotaxis. To assess the role of Rac1 in this process, we depleted Rac1 (Fig. S2M) and found that this too abrogated haptotaxis on fibronectin (Fig. 4A; Fig. S2N,Y). Depletion of Rac1 also significantly lowered velocity without altering persistence in our cells (Fig. S2O,Y). Recently, a putative oncogenic driver mutation in Rac1 has been identified – P29S – which leads to rapid GTPase cycling of Rac1 and constitutive activation of downstream pathways (Davis et al., 2013). To test whether enhanced Rac1 activity is also detrimental to a cells' ability to undergo haptotaxis, we created a conditionally activatable P29S knockin allele of the *Rac1* gene. We generated differentiated fibroblasts from embryonic stem cells where one copy of the gene of was replaced with the conditional mutation and triggered recombination with Cre. Expression of the Rac1 P29S mutation, from its endogenous promoter, blocked haptotaxis (Fig. 4B; Fig. S2P,Y). Rac1 P29S also lowered velocity without affecting persistence (Fig. S4Q,Y). Therefore, the proper regulation of Rac1, rather than simply the presence of Rac1-GTP, is important for controlling haptotaxis. To test whether Rac1 controls haptotaxis using differential protrusion dynamics, we performed kymography analysis on Rac1-depleted fibroblasts on a gradient of fibronectin. Depletion of Rac1 led to the loss of the differential protrusion dynamics seen in control haptotaxing fibroblasts (Fig. 4C; Fig. S2R), suggesting that Rac1 regulation of haptotaxis is through control of differential lamellipodial protrusion dynamics. Constitutively active Rac1 (P29S), depletion of Rac1 or inhibition of Rac1 GEFs (with NSC23766) all altered the localization of both WAVE2 and Arp2/3 (Fig. 4D,E; Fig. S2S), indicating that these perturbations are acting, at least in part, through the WRC–Arp2/3
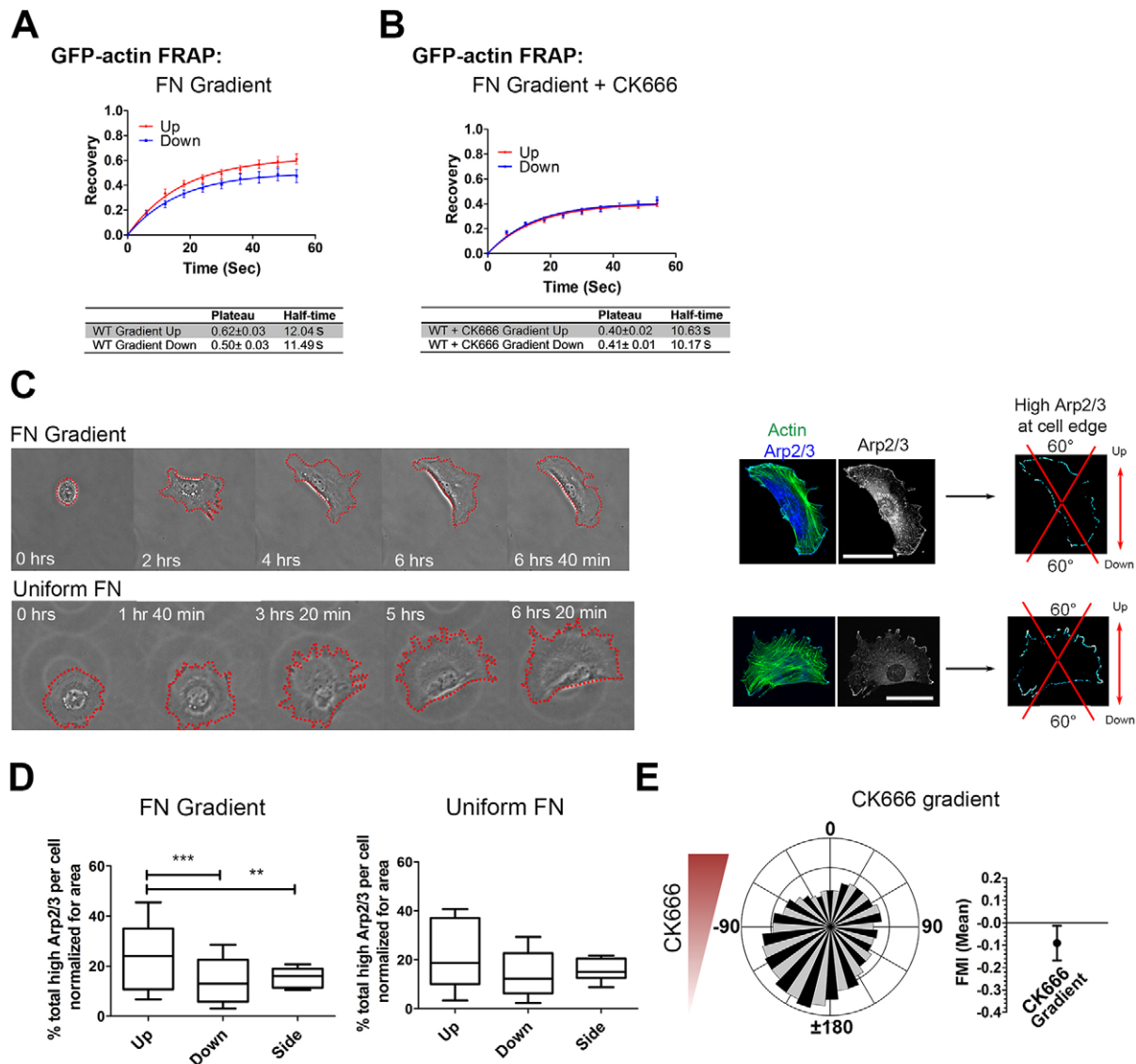
Fig. 2. Differential actin dynamics regulated through activity of the Arp2/3 complex is essential for haptotaxis on fibronectin. (A) FRAP of GFP–actin on a gradient of fibronectin (FN). Red=up and blue=down, mean±s.e.m. Tables display plateau (mean±s.e.m.) and half-life (mean) values with one-phase association, n=10. (B) FRAP of GFP–actin on a gradient of fibronectin with CK666 (150 µM) added for at least 3 h. Tables display plateau (mean±s.e.m.) and half-life (mean) values with one-phase association, n=18. (C) Correlative immunofluorescence analysis of actin (phalloidin) and Arp2/3 (Arpc2) staining in WT IA32 fibroblasts during haptotaxis or random migration (uniform fibronectin concentration, 10 µg/ml); phase images of the migrating cell with the corresponding immunofluorescence image are shown. Dotted red lines show the cell outline. Scale bars: 50 µm. Image of Arp2/3 (Arpc2) staining alone and the corresponding image of the high intensity Arp2/3 signal at the cell edge. The red lines show the division of the cell into 'up' (60°), 'down' (60°) and 'side' (240°, left and right) segments (relative to the gradient). Representative images from at least 20 cells. (D) Percentage of the high intensity Arp2/3 signal at the cell edge for each segment, normalized for area; in the box-and-whisker plots, the box represents the 25–75th percentiles, and the median is indicated. The whiskers show the 10–90th percentiles. Gradient of fibronectin: five chambers, 26 cells; uniform fibronectin: two chambers, 20 cells. (E) MTF migration on a gradient of CK666 – rose plot and FMI graph. The red triangle shows the direction of the CK666 gradient with respect to the rose plot. Data are mean±95% C.I.s. One-way ANOVA with Bonferroni's Multiple Comparison test, **P<0.01 and ***P<0.001.

pathway. Rac1 P29S fibroblasts exhibited increased WAVE2 and Arp2/3 localization at cell edges, as well as larger lamellipodial regions (Fig. 4D). Treatment with NSC23766 or knockdown of Rac1 resulted in less WAVE2 or Arp2/3 at the cell edge, coinciding with fewer lamellipodia (Fig. 4E; Fig. S2S). Taken together, our data suggest that appropriate Rac1 activation is essential for haptotaxis and that it controls this process through activation of WRC and Arp2/3 through regulation of lamellipodial dynamics.

Rac1 GEFs regulate the activity and localization of Rac1. Wash-in of NSC23766, a Rac GEF inhibitor (Gao et al., 2004), blocked fibroblast haptotaxis without affecting velocity or

persistence (Fig. 4F; Fig. S2T,Y). However, this inhibitor inhibits multiple Rac GEFs. β-Pix is a Rac1 GEF that functions at membrane ruffles and adhesions (Rosenberger and Kutsche, 2006). Based on previous cell spreading and migration studies (Kuo et al., 2011; Kutys and Yamada, 2014), β-Pix seemed to be a likely candidate for a GEF that is involved in haptotaxis. We depleted β-Pix (Fig. S2U) and observed that this did not affect haptotaxis, velocity or persistence (Fig. 4G; Fig. S2V,Y). Another Rac1 GEF that is inhibited by NSC23766, Tiam1, has been shown to play a role in membrane ruffles, lamellipodia and adhesions, as well as cell migration (Boissier and Huynh-Do, 2014; Wang et al., 2012; Nassar
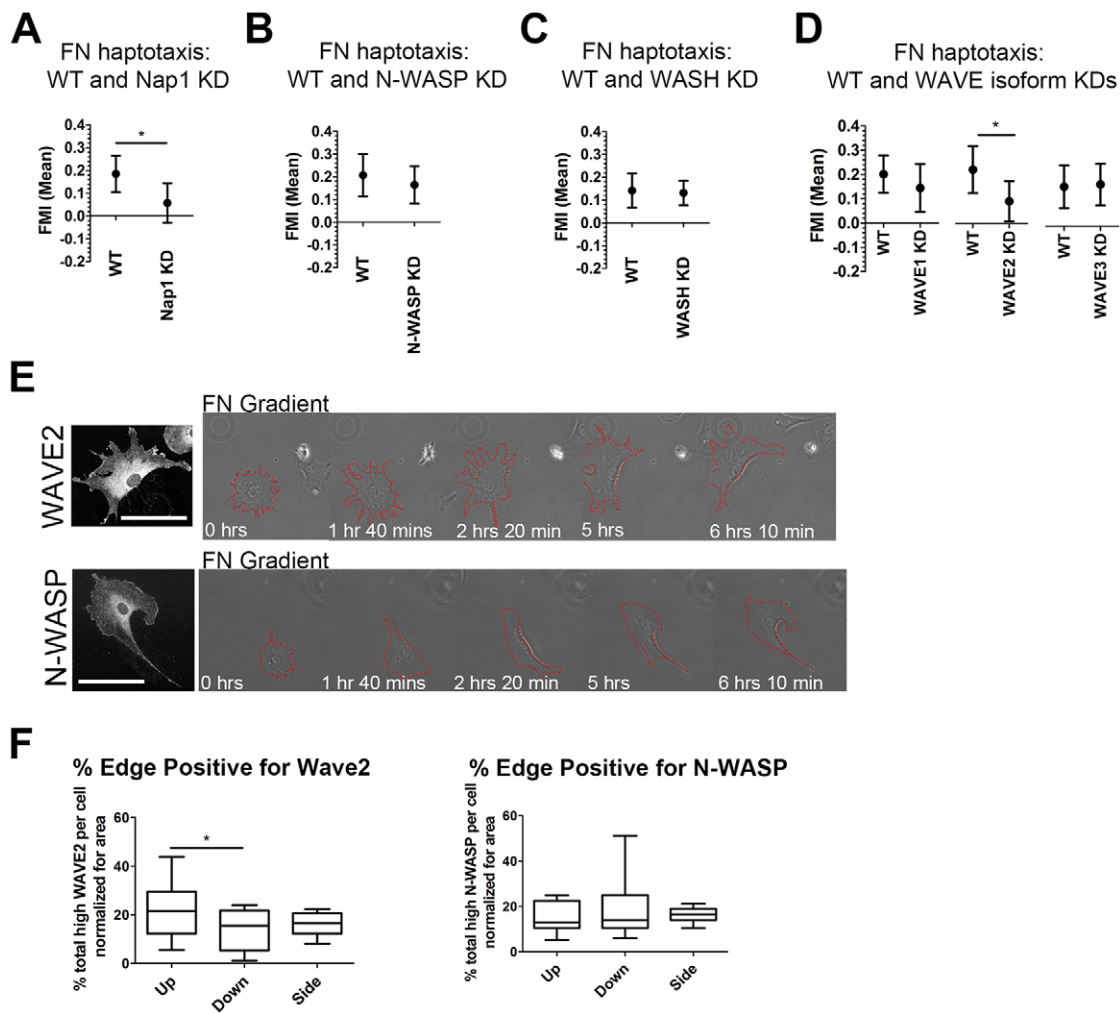
Fig. 3. The WRC, but not N-WASP or WASH, is the NPF required for haptotaxis on fibronectin. (A) FMI graph (mean±95% C.I.s) for haptotaxis on fibronectin (FN) of WT cells and cells transfected with shRNA1 against Nap1 (Nap1 KD). (B) FMI graph (mean±95% C.I.s) for haptotaxis on fibronectin of WT cells and cells transfected with shRNA1 against N-WASP (N-WASP KD). (C) FMI graph (mean±95% C.I.s) for haptotaxis on fibronectin of WT cells and cells transfected with shRNA1 against WASH (WASH KD). (D) FMI graph (mean±95% C.I.s) for haptotaxis on fibronectin of WT cells and cells transfected with shRNA1 against WAVE1, WAVE2 or WAVE3 (WAVE1, WAVE2 and WAVE3 KD, respectively). (E) Correlative immunofluorescence of WAVE2 or N-WASP staining during haptotaxis. Scale bar: 100 µm. Representative images from at least 17 cells. Red dashed lines outline cells. (F) Percentage of the high intensity WAVE2 or N-WASP signals at the cell edge for each segment, normalized for area; in the box-and-whisker plots, the box represents the 25–75th percentiles, and the median is indicated. The whiskers show the 10–90th percentiles. Cells were segmented into 'up' (60°), 'down' (60°) and 'side' (240°) segments. WAVE2: three chambers, 20 cells; N-WASP: four chambers, 17 cells. Student's t-tests (to compare two data sets) or one-way ANOVA with Bonferroni's Multiple Comparison test (to compare more than two data sets); *$P<0.05$.

et al., 2006). Depletion of Tiam1 (Fig. S2U) inhibited fibroblast haptotaxis while increasing cellular velocity, but it did not affect persistence (Fig. 4H; Fig. S2W,Y). Thus, Tiam1 is an essential GEF that regulates Rac1 to control haptotaxis.

FAK and SFK signaling at nascent adhesions and focal complexes, but not focal adhesions, is required for haptotaxis and regulates differential actin dynamics

Sites of adhesion where cells bind to the ECM range from small nascent adhesions to large stable focal adhesions. Rac1 and Tiam1 are localized at adhesion structures; therefore, we sought to test whether focal adhesions are required for haptotaxis. One treatment that ablates mature focal adhesions, but not nascent adhesions or focal complexes, is inhibition of Rho-kinase (ROCK, of which there are two isoforms ROCK1 and ROCK2), which leads to lower levels of myosin II activity. Treatment of fibroblasts with the ROCK inhibitor (Y-27632) depleted all internal focal adhesions and stress

fibers without disrupting the localization of the Arp2/3 complex (Fig. 5A). Interestingly, inhibition of ROCK did not affect haptotaxis (Fig. 5B; Fig. S3F) but did increase both the velocity and persistence of cells (Fig. S3A,F). Thus, our data suggest that mature focal adhesions do not seem to be required for fibroblast haptotaxis on fibronectin.

Focal complexes are the immature version of focal adhesions that form upon integrin activation. These structures also contain both Tiam1 and Rac1 (Boissier and Huynh-Do, 2014; Wang et al., 2012), along with clustered integrins, and are strong candidates for the adhesion structures required for haptotaxis in the place of mature focal adhesions. SFK and FAK signaling originates at focal complexes (Mitra and Schlaepfer, 2006) and, consistent with this, we observed active FAK and Src (phosphorylated FAK and Src) at focal complexes, as well as at lower levels at focal adhesions (Fig. 5C). Treatment with a FAK inhibitor (FAK inhibitor II; Slack-Davis et al., 2007) or SFK inhibitor (PP2; Hanke et al., 1996)
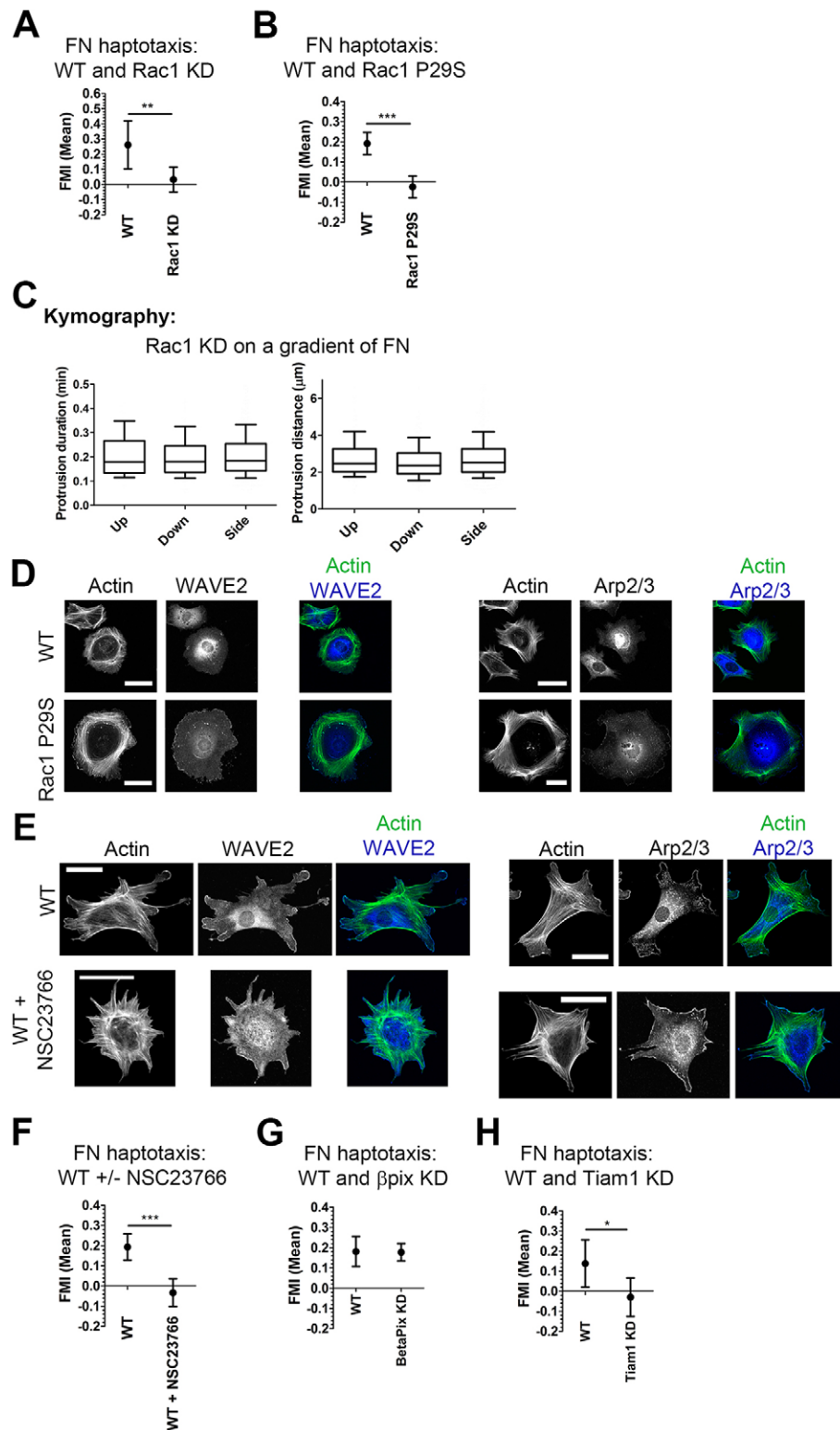
Fig. 4. Properly regulated Rac1 is essential for haptotaxis. (A) FMI graph (mean±95% C.I.s) for haptotaxis on fibronectin (FN) of WT and Rac1-knockdown (KD) shRNA1 IA32 fibroblasts. (B) FMI graph (mean±95% C.I.s) for haptotaxis on fibronectin of WT and Rac1-P29S fibroblasts. (C) Kymography analysis for Rac1-KD cells on a gradient of fibronectin. In the box-and-whisker plots, the box represents the 25–75th percentiles, and the median is indicated. The whiskers show the 10–90th percentiles. Four chambers, 26 cells. (D) Immunofluorescence for actin (phalloidin, green) with WAVE2 (blue) or Arp2/3 (Arpc2, blue) in WT and Rac1-P29S fibroblasts. Representative images from at least six cells. Scale bars: 50 µm. (E) Immunofluorescence for actin (phalloidin, green) with WAVE2 (blue) or Arp2/3 (Arpc2, blue) in cells±NSC23766 (200 µM). Representative images from at least three cells. Scale bars: 50 µm. (F) FMI graph (mean±95% C.I.s) for haptotaxis on fibronectin of cells with NSC23766 (200 µM) washed in. (G) FMI graph (mean±95% C.I.s) for haptotaxis on fibronectin of WT and β-Pix-KD cells. (H) FMI graph (mean±95% C.I.s) for haptotaxis on fibronectin of WT and Tiam1-KD shRNA1 cells. Student's t-tests (to compare two data sets) or one-way ANOVA with Bonferroni's Multiple Comparison test (to compare more than two data sets); *$P<0.05$, **$P<0.01$ and ***$P<0.001$.

decreased the activating phosphorylation of FAK and Src (without altering the total levels), respectively, and also altered the localization of the adhesions (Fig. S3B). Consistent with the hypothesized role of focal complex signaling during haptotaxis, inhibition of either FAK or SFKs blocked haptotaxis while decreasing both velocity and persistence (Fig. 5D; Fig. S3C,F). Furthermore, fibroblasts that lacked all SFKs [Src, Yes and Fyn; SYF-null mouse embryonic fibroblasts (MEFs) (Klinghoffer et al.,

1999)] could not undergo haptotaxis, whereas re-expressing Src in SYF-null MEFs restored haptotaxis (Fig. 5E; Fig. S3D–F). FAK and SFK signaling has also been implicated in leading edge actin dynamics through WRC and Tiam1 activation (Ardern et al., 2006; Chen et al., 2010; Servitja et al., 2003), as well as in the formation of a direct association of FAK with the Arp2/3 complex (Serrels et al., 2007; Swaminathan et al., 2016). Based on these studies and our data, we hypothesized that SFK signaling is an upstream regulator of
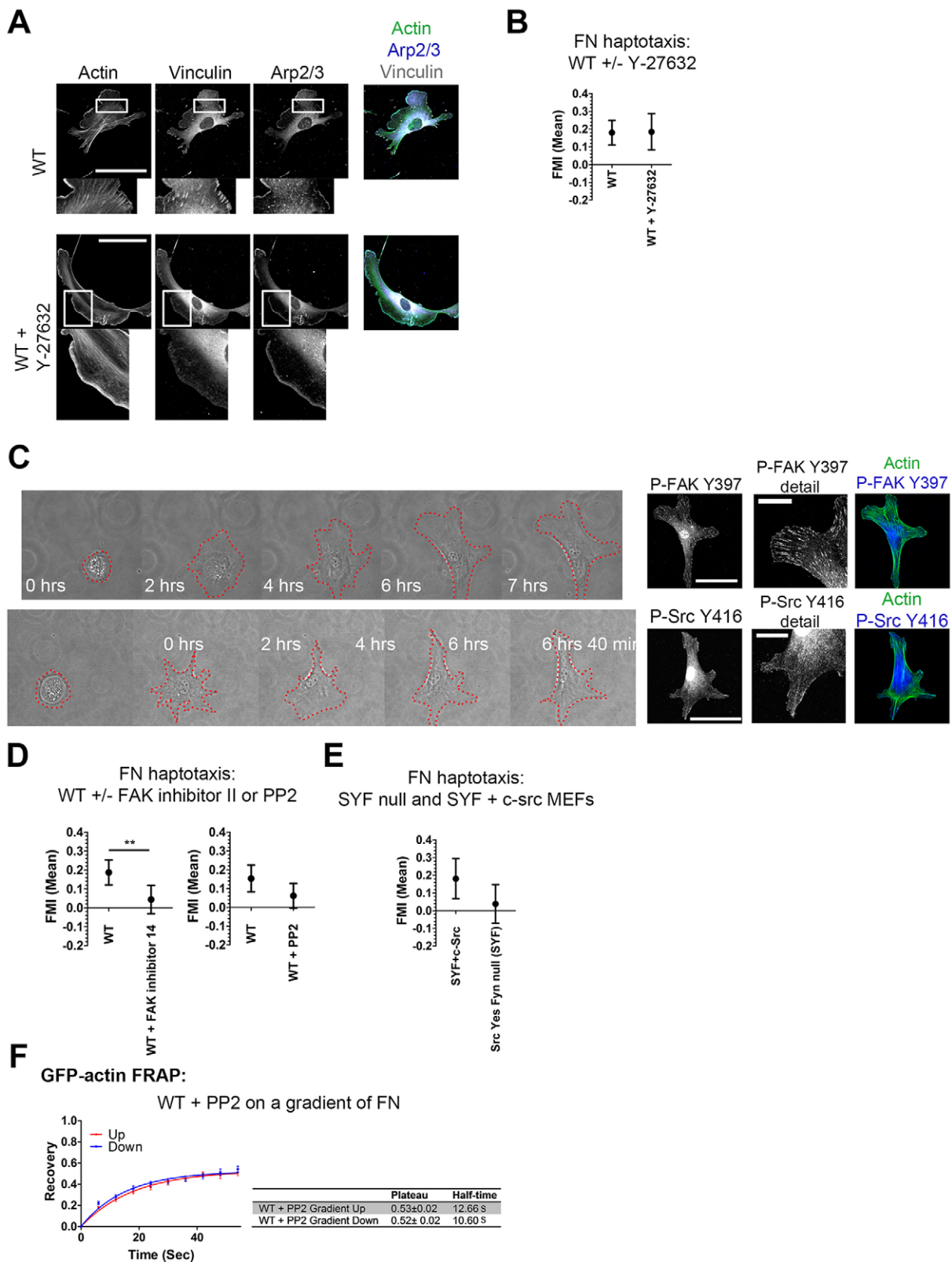
Fig. 5. Focal adhesions are dispensable for haptotaxis, whereas FAK and SFKs are required and affect differential actin dynamics.
(A) Immunofluorescence staining for actin (phalloidin, green), vinculin (grey) and Arp2/3 (Arpc2, blue) in WT and Y-27632-treated (15 μM) IA32 fibroblasts. Representative images from at least five cells. Scale bars: 100 μm. (B) FMI graph (mean±95% C.I.s) for haptotaxis on fibronectin (FN) of cells with Y-27632 (15 μM) washed in. (C) Correlative immunofluorescence of phosphorylated (p)-FAK at residue Y397 or phosphorylated (p)-Src at residue Y416 in WT IA32 fibroblasts during haptotaxis. Red dashed lines outline cells. Scale bars: 100 μm (main images); 30 μm (detail images). Representative images from at least nine cells. (D) FMI graph (mean±95% C.I.s) for haptotaxis on fibronectin of cells with either FAK inhibitor II (10 μM) or PP2 (10 μM) washed in. (E) FMI graph (mean±95% C.I.s) for haptotaxis on fibronectin of SYF-null and SYF-null+Src (rescue) MEFs. (F) FRAP of GFP–actin in cells on a gradient of fibronectin with PP2 (10 μM) added for at least 3 h. Table displays plateau (mean+s.e.m.) and half-life (mean) values with one-phase association; 14 cells. Student's t-test, **P<0.01.

the differential actin dynamics observed in cells undergoing haptotaxis. Treatment with PP2 on a gradient of fibronectin led to the loss of the differential actin dynamics seen in fibroblasts as measured using FRAP analysis of GFP–actin (Fig. 5F), indicating that the requirement for SFK in haptotaxis operates, at least in part, by regulating WRC and Arp2/3, leading to differential actin and protrusion dynamics at the leading edge.

Fibroblasts rely primarily on β1-containing integrins for fibronectin haptotaxis

Integrins are the primary receptor for ECM, and the main integrin β subunits that bind to fibronectin in fibroblasts are β1, β3 and β5 (encoded by *ITGB1*, *ITGB3* and *ITGB5*, respectively). To test whether a specific β integrin is responsible for regulating haptotaxis in fibroblasts, we studied fibronectin haptotaxis using β1- and β3-null MEFs with rescue derivatives (β1–GFP or β3–GFP re-expressed to endogenous levels; called β1–GFP and β3–GFP MEFs, respectively) (Parsons et al., 2008; Worth et al., 2010; King et al., 2011). These MEFs express low levels of β5 integrin; therefore, depletion of this subunit was not necessary (Fig. S3G). Lack of β3 integrin did not affect haptotaxis but decreased velocity and increased persistence (Fig. 6A; Fig. S3H,M). To extend this result, we also used cilengitide (a β3- and β5-integrin-specific cyclic peptide inhibitor) (Desgrosellier and Cheresh, 2010). Treatment with cilengitide at concentrations of $\geq$10 μM caused fibroblasts to

detach from fibronectin, precluding any analysis of haptotaxis. To circumvent this, we backfilled the fibronectin gradient surface with poly-L-lysine (PLL) to allow the cells to remain adherent and motile, even without integrin adhesion. Treatment of β1–GFP MEFs with cilengitide caused a trend towards reduced haptotactic fidelity, suggesting a partial role of β3 integrin either directly or through its regulation of β1 integrin in the regulation of haptotaxis (Fig. 6B; Fig. S3M). Additionally, this results in a decrease in persistence but no change in velocity (Fig. S3I,M). Cells that lacked β1 integrin also showed a decreased haptotactic response, without alteration in velocity or persistence (Fig. 6B; Fig. S3I,M). However, treatment of β1-null MEFs with cilengitide, which inhibits all remaining fibronectin-binding integrins, completely abrogated haptotaxis while decreasing persistence but not altering velocity (Fig. 6B; Fig. S3I,M). These data indicate that β3-containing integrins can partially substitute for β1-containing integrins during haptotaxis, but that the main integrins responsible for fibronectin haptotaxis are the β1-containing integrins.

FRAP analysis of β1–GFP in MEFs undergoing haptotaxis did not show differential turnover of the β1 integrin at the cell edge extending up gradient compared to that down the gradient, and there was no obvious differential distribution of active β1 integrin in MEFs undergoing haptotaxis (Fig. 6C,D). Therefore integrins, and β1-containing integrins in particular, are necessary for haptotaxis but are not differentially localized. Kindlins and talin activate
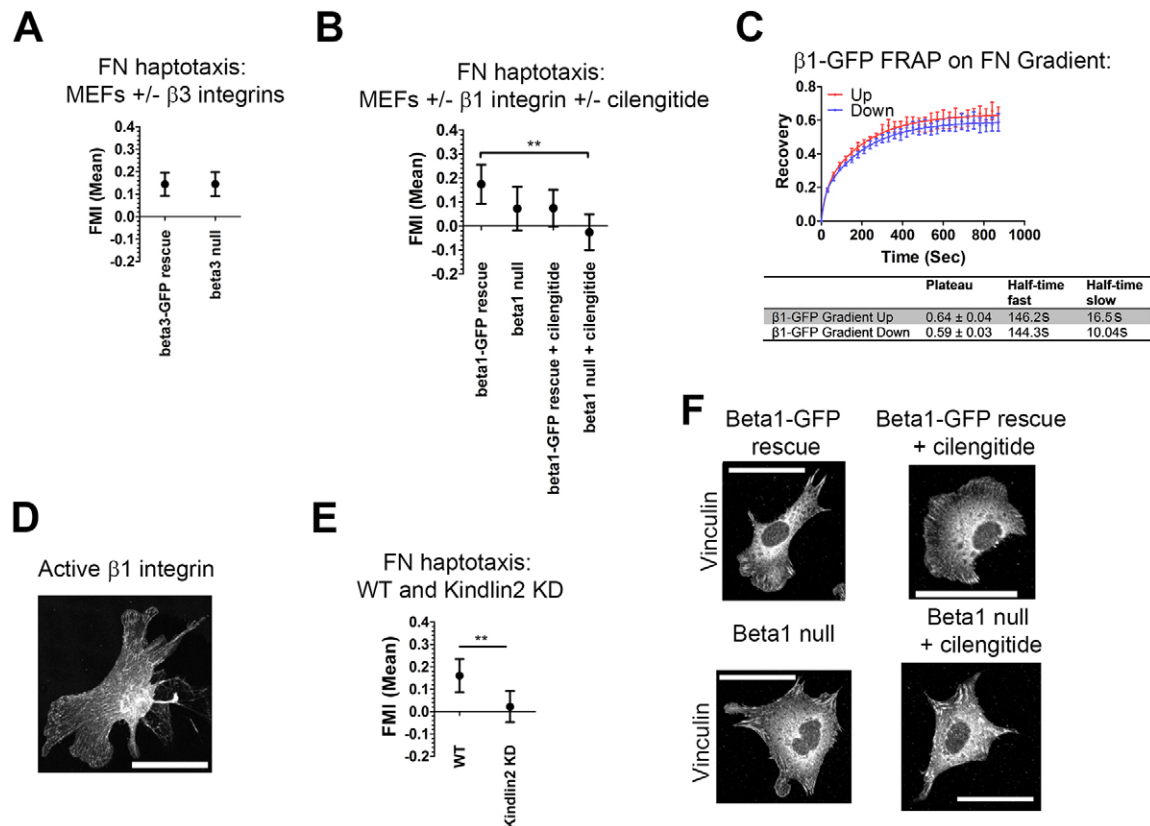

	Plateau	Half-time fast	Half-time slow
β1-GFP Gradient Up	0.64 ± 0.04	146.2S	16.5S
β1-GFP Gradient Down	0.59 ± 0.03	144.3S	10.04S

Fig. 6. Haptotaxis on fibronectin is an integrin-based process. (A) FMI graph (mean±95% C.I.s) for haptotaxis on fibronectin (FN) of β3-null MEFs and the rescue line (expressing β3–GFP). (B) FMI graph (mean±95% C.I.s) for haptotaxis on fibronectin (backfilled with 125 μg/ml PLL) of β1-null MEFs±β1–GFP (rescue)±cilengitide (40 μM). (C) FRAP analysis of β1–GFP in β1–GFP MEFs on a gradient of fibronectin. Table displays plateau (mean±s.e.m.) and half-life (mean) values with two-phase association; ten cells. (D) Correlative immunofluorescence of staining for active β1 integrin in WT IA32 fibroblasts during haptotaxis. Representative image from 31 cells. (E) FMI graph (mean±95% C.I.s) for haptotaxis on fibronectin of WT and kindlin2-KD shRNA1 cells. (F) Immunofluorescence staining for vinculin of β1-null MEFs±β1–GFP (rescue)±cilengitide (40 μM) on fibronectin (100 μg/ml) and PLL (75 μg/ml). Representative images from at least four cells. Scale bars: 50 μm. Student's *t*-tests (to compare two data sets) or one-way ANOVA with Bonferroni's Multiple Comparison test (to compare more than two data sets); **P<0.01.

integrins, and kindlin2 has been shown to associate with β1 integrin at nascent adhesions before talin recruitment during adhesion maturation (Bachir et al., 2014). Consistent with a central role of β1-containing integrins, depletion of kindlin2 in fibroblasts (Fig. S3J) blocked haptotaxis without altering either velocity or persistence (Fig. 6E; Fig. S3K–M), suggesting that kindlin2 activates β1-containing integrins during fibronectin haptotaxis.

A crucial aspect of integrin function is their spatial organization within the membrane. Several different structures contain clustered integrins ranging from small transient nascent adhesions to large stable focal adhesions. Consistent with previous findings (King et al., 2011; Parsons et al., 2008), adhesions appeared to be altered in cells that lacked β1 integrin, and treatment of either β1–GFP or β1-null MEFs with cilengitide led to smaller adhesions in β1–GFP MEFs and fewer adhesions at the cell edge in β1-null MEFs, as visualized with staining of vinculin (Fig. 6F).

The Rac–WRC–Arp2/3 pathway also regulates haptotaxis in 3D fibronectin gradients

Although studies of 2D cell migration have been highly productive, questions about the relevance of mechanisms elucidated in 2D migration for the more physiological 3D migration remain. To

address this, we probed the mechanism of haptotaxis in 3D collagen gels. In this environment, Arp2/3- and actin-positive protrusions could readily be observed in KOR cells (Fig. 7A). 3D haptotaxis fibronectin gradients can be formed by plating fibroblasts inside the central chamber of our microfluidics chamber in 3D collagen gels (Chan et al., 2014). Fluorescent fibronectin is then added through the source channel, whereby it forms a gradient across the collagen gel that interacts with the fibrils. Unbound fibronectin is then flushed out of the chamber, leaving only collagen fibril-bound fibronectin in a gradient (Fig. S4A). To test the requirement for Arp2/3 in 3D haptotaxis, we used our $Arpc2$ conditional knockout cells. WT MTFs haptotax towards the higher concentration of fibronectin inside the 3D collagen gel, whereas $Arpc2^{-/-}$ MTFs did not (Fig. 7B; Fig. S4H). $Arpc2^{-/-}$ MTFs also moved with lower velocities and persistence than their WT counterparts (Fig. S4B,H). Our 2D studies implicated the WRC as the key NPF required for haptotaxis. To investigate whether the WRC is also required for 3D haptotaxis, as it is for 2D haptotaxis, WT MTFs were depleted of Nap1 (Fig. S4C). Nap1-depleted MTFs did not haptotax on 2D fibronectin gradients (Fig. S4D,H; corroborating our results with IA32 fibroblasts) or 3D fibronectin gradients (Fig. 7C; Fig. S4H). No effect on velocity was observed in either two dimensions or three
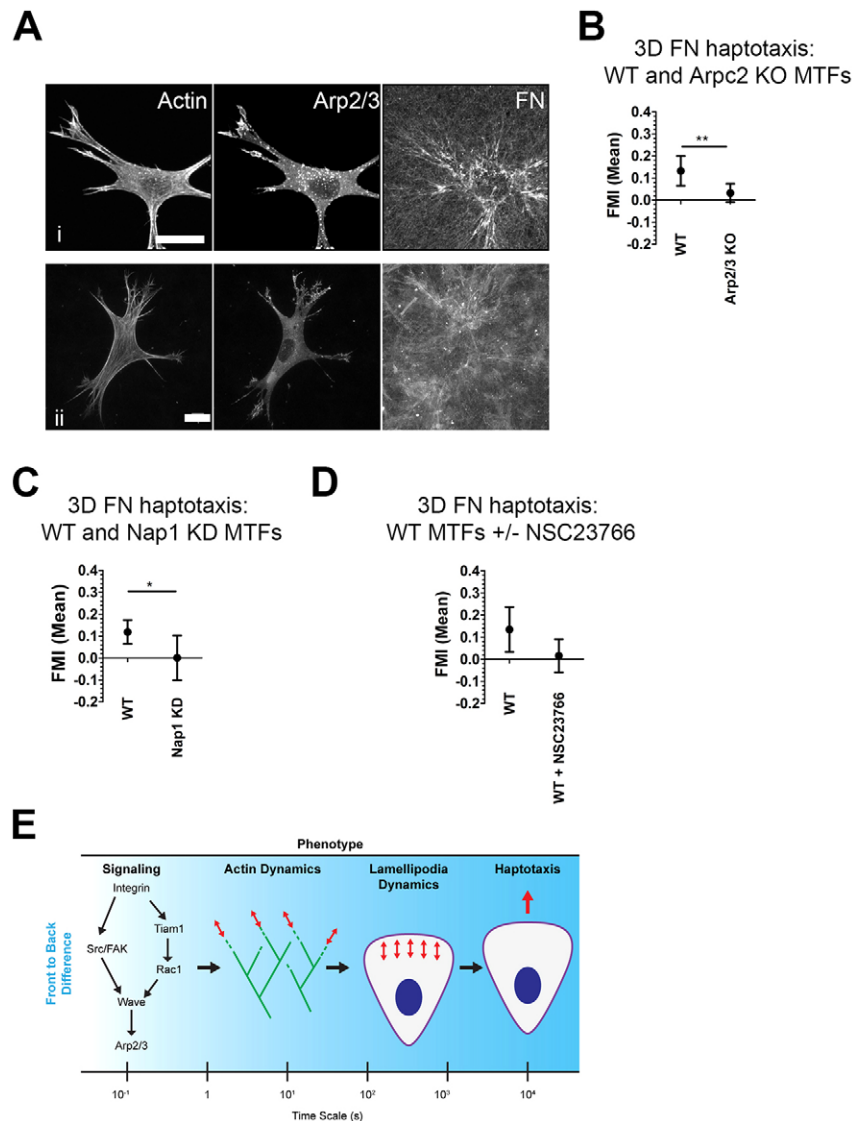

Fig. 7. The Rac1–WRC–Arp2/3 pathway that is essential for 2D haptotaxis on fibronectin is also required for 3D haptotaxis. (A) Immunofluorescence of MTF $Arpc2^{-/-}$+Arpc2–GFP (Arpc2 KO rescue, KOR) in a 3D collagen and Cy5–fibronectin gel, stained for actin (phalloidin). (i) confocal plus AiryScan; (ii) standard confocal. Representative images from at least three cells. Scale bars: 20 µm. (B) FMI graph (mean±95% C.I.s) for 3D haptotaxis in fibronectin (500 µg/ml Cy5–fibronectin source through a collagen gel) of WT and $Arpc2^{-/-}$ (Arp2/3 KO) MTFs. (C) FMI graph (mean±95% C.I.s) for 3D haptotaxis in fibronectin of WT and Nap1-KD MTFs. (D) FMI graph (mean±95% C.I.s) for 3D haptotaxis in fibronectin of cells treated with and without NSC23766 (200 µM). (E) Scheme of the haptotaxis pathway in response to fibronectin. Student's t-test; *$P<0.05$, **$P<0.01$. Red arrow indicates direction of migration, double headed red arrows indicate dynamics processes.

dimensions; however, persistence was increased with Nap1 depletion during 3D haptotaxis (Fig. S4E,H). Inhibition of Rac GEFs with NSC23766 blocked MTF haptotaxis on 2D fibronectin (Fig. S4F,H; as seen with IA32 fibroblasts) and 3D fibronectin gradients. This treatment also decreased velocity with no change in persistence in 3D gradients (Fig. 7D; Fig. S4G,H). Taken together, these data suggest that the same pathway is operating to regulate fibroblast haptotaxis in 3D collagen–fibronectin gels as on 2D fibronectin surfaces.

DISCUSSION
A working model for haptotaxis
Our results provide substantial insight into the cellular and molecular mechanisms of haptotaxis, leading us to develop a working model of this process (Fig. 7E). Cells encountering a gradient in the ECM (i.e. in the concentration of fibronectin, laminin, etc) trigger a pathway initiated by the clustering and activation of integrins at nascent adhesions and/or focal complexes. This prompts the activation of FAK, SFK and Rac signaling, which converge on the WRC to promote activation of the Arp2/3 complex. It remains to be determined whether FAK and SFK, and Rac act in parallel or series in this pathway. WRC-based activation of the Arp2/3 complex leads to formation of lamellipodia. These lamellipodia protrude in all directions but are reinforced when they protrude up the gradient towards higher concentrations of ECM (e.g. increased concentration of fibronectin). We postulate that this constitutes a positive-feedback loop whereby lamellipodia protruding up gradient engage more integrins, which in turn triggers augmented signaling through this pathway and further protrusion. It is important to note that this spatial aspect of the model cannot be effectively modeled by simply plating cells onto uniform ECMs with different concentrations of components, and requires the use of gradients. Remarkably, cells can sense and respond to fairly shallow gradients of ECM, implying that amplification of the input signal must be occurring. Future studies will be directed towards trying to understand the nature of this amplification.

An important aspect of this model is the concept that the summation of small differences in actin and lamellipodial dynamics over time can yield substantial directional cell migration. The signaling events connecting integrins to the Arp2/3 complex are happening rapidly in the sub-second to second timescale. This pathway leads to more dynamic actin and longer lasting lamellipodial protrusions in the direction of higher concentrations of ECM in the order of seconds to minutes. Finally, these differential protrusion dynamics lead to differential whole-cell movement towards higher concentrations of ECM over the course of hours. Small differences across a cell in the signaling pathways and protrusion dynamics are summed over time, leading to larger differences in cell movement and, ultimately, the haptotactic response. This might be a unique feature of slow moving mesenchymal cells such as fibroblasts, but it could also be a useful paradigm for studying directional migration in other contexts, such as in 1 dimensional migration, collective migration of epithelial cells or the invasion of tumor cells (Chan et al., 2014).

This model also highlights the diversity of mechanisms involved in directional cell migration (Bear and Haugh, 2014). Unlike chemotaxis, where cells can perceive the directional cue passively via diffusion, haptotaxis requires that cells protrude or migrate towards a fixed substrate-bound cue. In addition to differences in the presentation and sensing of the cue, haptotaxis clearly has a different set of required molecular components to chemotaxis. For example, N-WASP is dispensable for haptotaxis but is required

for chemotaxis (King et al., 2011). Conversely, Rac1 is necessary for haptotaxis but is dispensable for chemotaxis (Monypenny et al., 2009). In addition, we have recently mapped the pathway that fibroblasts use to sense and respond to PDGF gradients, which involves PLCγ and PKCα, and the local inactivation of myosin IIA at the leading edge of cells (Asokan et al., 2014). These observations, along with our original observations that Arp2/3-depleted cells can undergo chemotaxis but not haptotaxis (Wu et al., 2012), strongly suggest that haptotaxis and chemotaxis operate through distinct pathways.

Lamellipodia and the signaling events that trigger them are required for haptotaxis
Several lines of evidence indicate that the Arp2/3 complex is required for haptotaxis, but its cellular mechanism of action during haptotaxis was not clear until this study. Activation of Arp2/3 by NPFs leads to the formation of branched actin at several locations in cells. By depleting NPFs associated with specific structures, we were able to narrow our search to the lamellipodia generated by the WRC. This conclusion was supported by the finding that WAVE2 (but not N-WASP) preferentially localizes to the side of haptotaxing cells that is closest to the up gradient. Other Arp2/3-dependent processes, such as endocytosis and retromer trafficking, might play accessory roles in haptotaxis, but these are not required in the same way that WRC-driven lamellipodia are. Recent data from our group also indicate that the Arp2/3 debranching factor GMFβ is crucial for haptotaxis (Haynes et al., 2015), suggesting that proper tuning of branched actin dynamics, not just their presence, is required for haptotaxis. Furthermore, recent work indicates that the actin bundling protein fascin is required for haptotaxis, probably through its role in filopodia, which frequently form the template for future lamellipodia (Johnson et al., 2015).

To sense and respond to the ECM gradient during haptotaxis, cells must engage the ECM through integrins. Our data indicate that β1-containing integrins are the primary adhesive receptors for fibronectin haptotaxis, but that β3-containing integrins can partially compensate for the loss of β1 integrin. It is certainly possible that other receptors for fibronectin, such as syndecans enhance haptotactic responses, but they do not appear to be sufficient to support haptotaxis without integrins. Our data also speak to the spatial arrangement of integrins during haptotaxis. The lamellipodium is a site for the generation of nascent adhesion structures, focal complexes and the maturation of a subset of these into the larger focal adhesions. Our results point to focal complexes but not to mature focal adhesions as the regulators of fibronectin haptotaxis. Inhibiting ROCK leads to the loss of mature focal adhesions; however, these cells can still consistently undergo haptotaxis. Rac1, Tiam1, SFKs and FAK all localize to focal complexes (Mitra and Schlaepfer, 2006; Rottner et al., 1999; Wang et al., 2012), and are all required for haptotaxis, further implicating focal complexes as the main adhesion complex required for fibronectin haptotaxis. Because many other cell types that lack mature focal adhesions exhibit integrin-containing structures similar to focal complexes, haptotactic responses might be a characteristic of many cell types (Weber et al., 2013).

The relevance of haptotaxis for tumor progression and metastasis
Tumor cells encounter a variety of ECM environments as malignancies progress from local tumors to metastatic disease. In many cases, the stromal response to tumors manifests as changes in the amount, alignment and/or degradation of ECM (Schedin and

Keely, 2011). Some of the earliest literature on haptotaxis postulates that this process is crucial for tumor progression (Carter, 1968). It is striking that almost every component in the fibroblast haptotaxis pathway we have uncovered has been linked to tumor progression. FAK and SFKs have well-described roles in tumor behavior (Mitra and Schlaepfer, 2006). Rac1 and upstream regulators such as Tiam1 have also been linked to the aggressiveness of tumors (Boissier and Huynh-Do, 2014). Rac1 levels are shown to inversely correlate with poor prognosis in a number of tumors, and depletion of Rac1 decreases cell invasion both *in vitro* and *in vivo* (Alan and Lundquist, 2013). Furthermore, an activating mutation in Rac1, Rac1 P29S, has been linked to disease progression and metastasis in melanoma (Mar et al., 2014), and clearly blocks haptotaxis in fibroblasts in response to fibronectin. Finally, mutations in Cyfip1, a subunit of the WRC, implicate it as an invasion-suppressor protein in epithelial cancer (Silva et al., 2009).

We were encouraged to look for a connection between haptotaxis and tumor invasion because of our previous work on the tumor suppressor LKB1. In that work, we demonstrated that loss of LKB1 and its direct downstream target MARK in melanoma leads to the loss of haptotaxis and of more invasive migration phenotypes (Chan et al., 2014). Tumor cells are known to ignore tissue boundaries, and failure to sense differences in the ECM could be one mechanism by which they ignore these boundaries. The mapping of the fibroblast haptotactic pathway presented in this work has only reinforced this view through the identification of factors that have already been implicated in tumor progression and metastasis. Taken together, these data suggest that it will be crucial to understand the mechanisms of haptotactic sensing and response in order to develop new therapeutic options for metastatic cancer and other human diseases involving inappropriate cell migration.

MATERIALS AND METHODS
Materials, reagents and cell lines
Commercial antibodies, sources and details on usage are found in Table S1. Chemicals, sources and details on usage are found in Table S2. Cell lines with details on culture conditions are found in Table S3.

Lentivirus
Lentivirus production and infection were as described previously (Cai et al., 2008). Bulk populations of IA32 fibroblasts or MTFs were transduced with lentivirus and selected with 2 µg/ml puromycin (IA32 fibroblasts) or 200 µg/ml hygromycin (MTFs) for 2 days. Western blotting was performed to assess knockdown efficiency; cells were utilized for experiments for 4–7 days after infection. Sequences of the shRNAs used are found in Table S4.

Western blotting
Western blotting was performed as described previously (Haynes et al., 2015).

Haptotaxis chamber procedures
Microfluidic device preparation and haptotaxis gradient experiments were performed as described previously (Wu et al., 2012). Addition of 250 µg/ml Cy5–fibronectin (for IA32 fibroblasts) or 500 µg/ml Cy5–fibronectin (for other cell lines) to the source channel created a gradient across the central channel through diffusion. The gradient was visualized and confirmed using a line scan as previously described (Wu et al., 2012; Chan et al., 2014). Two methods have been developed to control for gradient differences between chambers. RNAi or overexpression cell lines are plated in the central chamber alongside wild-type control cells (labeled with two different fluorophores in order to differentiate the two sets). Additionally, a wash-in protocol has been developed (previously described by Chan et al., 2014) to allow matched comparison of non-drug treatment versus drug-treated

cells. A wash-in of DMSO as a vehicle control did not alter haptotaxis or any other metric of migration (Fig. S1A,B,L). For PLL backfilling experiments, Cy3–poly-L-lysine (125 µg/ml) was added to the central chamber after the fibronectin to provide adhesion sites. 3D haptotaxis chambers were set up as described previously (Chan et al., 2014). Cells were plated in 1 mg/ml acid-neutralized collagen into the central channel of our microfluidics chamber, after which the fibronectin gradient was formed as described for 2D haptotaxis.

Migration analysis
Haptotaxis assays were imaged using the VivaView FL microscope with a 20× objective and a motorized magnification changer set to ×0.5. Cells were imaged every 10 min for >12 h, fluorescence images to differentiate cell types were taken as the first image. Individual cells were manually tracked using ImageJ software (Manual Tracking plugin), with cells in both two and three dimensions being tracked in the x–y axis. The tracks obtained were further analyzed using the Chemotaxis and Migration Tool plugin (ibidi) to extract the FMI, velocity and persistence of cell tracks. Metrics were analyzed using Prism (GraphPad Software) and displayed as mean±95% confidence intervals, or box and whisker plots with 10–90 percentiles. Statistical analysis was subsequently performed using *t*-tests. Rose plots of directional migration on normalized polar coordinates were generated using a MATLAB (MathWorks) script (trackingangleshistv14). For random migration on uniform fibronectin, glass-bottomed dishes (MatTek) were cleaned with plasma for 2 min and coated with fibronectin at 10 µg/ml for 5–10 min at 37°C, if the dishes were not cleaned with plasma, they were coated with fibronectin for 1 h at 37°C. Subsequently, the dishes were rinsed in PBS three times, and then cells were plated onto the coated dishes.

Subcellular analysis
Cells were stained for immunofluorescence as described previously (Bear et al., 2002). For correlative immunofluorescence, live cells were observed undergoing haptotaxis or random migration, which was followed by fixation and staining with specific antibodies using our standard immunofluorescence protocol. Imaging was performed using an Olympus FV1000 or FV1200 confocal microscope, controlled by Fluoview, with a ×40 1.3 NA Olympus objective. Images displayed are maximum intensity *z*-stack projections. Imaging of the 3D collagen–Cy5 fibronectin gels were performed using a Zeiss 880 instrument with or without Airyscan, with a ×63 1.4 NA objective. Edge intensity measurements were performed as described previously (Haynes et al., 2015). FRAP was performed on GFP–actin-expressing IA32 fibroblasts or β1–GFP MEFs in the haptotaxis chambers or on random migration dishes. Cells were plated in a haptotaxis chamber or random migration dish and allowed to migrate for 4 h before imaging. Analysis was performed on normalized data (pre-bleach=1, bleach=0) using Prism (GraphPad Software) with one-phase (GFP–actin) or two-phase (β1–GFP) association. Kymography was performed as described previously (Haynes et al., 2015). For correlative immunofluorescence, FRAP and kymography, cells on haptotactic gradients were segmented into 'up' (60°), 'down' (60°) and 'side' (240°) regions, and the various metrics from these regions were calculated separately.

Light-activated protrusion
IA32 fibroblasts were sorted for stable expression of Venus-iLID-CAAX and Tiam1 DH/PH-tgRFPt-Micro (Guntas et al., 2015) and then plated in a haptotactic fibronectin chamber. Induction of recruitment of Tiam DH/PH-tgRFPt-Micro to localized areas of the membrane and imaging was performed as previously described (Guntas et al., 2015). During activation, two equally sized (40×40 pixels) regions of interest (ROI) were activated with 1% power of the 488-nm laser. The ROIs were positioned at morphologically similar cell edges up and down the gradient of fibronectin. Images were analyzed by generating kymographs through the center of each ROI using FIJI (ImageJ) software. Each kymograph was then traced in FIJI, and the position of the cell edge at each time point was interpolated from the traces. Protrusion and retraction data were plotted by first normalizing the curves to the previous five positions and averaging all up- and down-gradient traces. Curves were fit using Prism statistical software.

Supplementary information
Supplementary information available online at
http://jcs.biologists.org/lookup/doi/10.1242/jcs.184507.supplemental

References

Alan, J. K. and Lundquist, E. A. (2013). Mutationally activated Rho GTPases in cancer. *Small GTPases* **4**, 159-163.

Ardern, H., Sandilands, E., Machesky, L. M., Timpson, P., Frame, M. C. and Brunton, V. G. (2006). Src-dependent phosphorylation of Scar1 promotes its association with the Arp2/3 complex. *Cell Motil. Cytoskeleton* **63**, 6-13.

Asokan, S. B., Johnson, H. E., Rahman, A., King, S. J., Rotty, J. D., Lebedeva, I. P., Haugh, J. M. and Bear, J. E. (2014). Mesenchymal chemotaxis requires selective inactivation of myosin II at the leading edge via a noncanonical PLCgamma/PKCalpha pathway. *Dev. Cell* **31**, 747-760.

Aznavoorian, S., Stracke, M. L., Krutzsch, H., Schiffmann, E. and Liotta, L. A. (1990). Signal transduction for chemotaxis and haptotaxis by matrix molecules in tumor cells. *J. Cell Biol.* **110**, 1427-1438.

Bachir, A. I., Zareno, J., Moissoglu, K., Plow, E. F., Gratton, E. and Horwitz, A. R. (2014). Integrin-associated complexes form hierarchically with variable stoichiometry in nascent adhesions. *Curr. Biol.* **24**, 1845-1853.

Bear, J. E. and Haugh, J. M. (2014). Directed migration of mesenchymal cells: where signaling and the cytoskeleton meet. *Curr. Opin. Cell Biol.* **30**, 74-82.

Bear, J. E., Svitkina, T. M., Krause, M., Schafer, D. A., Loureiro, J. J., Strasser, G. A., Maly, I. V., Chaga, O. Y., Cooper, J. A., Borisy, G. G. et al. (2002). Antagonism between Ena/VASP proteins and actin filament capping regulates fibroblast motility. *Cell* **109**, 509-521.

Boissier, P. and Huynh-Do, U. (2014). The guanine nucleotide exchange factor Tiam1: a Janus-faced molecule in cellular signaling. *Cell. Signal.* **26**, 483-491.

Cai, L., Makhov, A. M., Schafer, D. A. and Bear, J. E. (2008). Coronin 1B antagonizes cortactin and remodels Arp2/3-containing actin branches in lamellipodia. *Cell* **134**, 828-842.

Campellone, K. G. and Welch, M. D. (2010). A nucleator arms race: cellular control of actin assembly. *Nat. Rev. Mol. Cell Biol.* **11**, 237-251.

Carter, S. B. (1965). Principles of cell motility: the direction of cell movement and cancer invasion. *Nature* **208**, 1183-1187.

Carter, S. B. (1968). Tissue homeostasis and the biological basis of cancer. *Nature* **220**, 970-974.

Chan, K. T., Asokan, S. B., King, S. J., Bo, T., Dubose, E. S., Liu, W., Berginski, M. E., Simon, J. M., Davis, I. J., Gomez, S. M. et al. (2014). LKB1 loss in melanoma disrupts directional migration toward extracellular matrix cues. *J. Cell Biol.* **207**, 299-315.

Chen, Z., Borek, D., Padrick, S. B., Gomez, T. S., Metlagel, Z., Ismail, A. M., Umetani, J., Billadeau, D. D., Otwinowski, Z. and Rosen, M. K. (2010). Structure and control of the actin regulatory WAVE complex. *Nature* **468**, 533-538.

Clark, R. A. F. (1990). Fibronectin matrix deposition and fibronectin receptor expression in healing and normal skin. *J. Invest. Dermatol.* **94**, 128s-134s.

Davis, M. J., Ha, B. H., Holman, E. C., Halaban, R., Schlessinger, J. and Boggon, T. J. (2013). RAC1P29S is a spontaneously activating cancer-associated GTPase. *Proc. Natl. Acad. Sci. USA* **110**, 912-917.

Desgrosellier, J. S. and Cheresh, D. A. (2010). Integrins in cancer: biological implications and therapeutic opportunities. *Nat. Rev. Cancer* **10**, 9-22.

Gao, Y., Dickerson, J. B., Guo, F., Zheng, J. and Zheng, Y. (2004). Rational design and characterization of a Rac GTPase-specific small molecule inhibitor. *Proc. Natl. Acad. Sci. USA* **101**, 7618-7623.

Guntas, G., Hallett, R. A., Zimmerman, S. P., Williams, T., Yumerefendi, H., Bear, J. E. and Kuhlman, B. (2015). Engineering an improved light-induced dimer (iLID) for controlling the localization and activity of signaling proteins. *Proc. Natl. Acad. Sci. USA* **112**, 112-117.

Halaban, R. (2015). RAC1 and melanoma. *Clin. Ther.* **37**, 682-685.

Hanke, J. H., Gardner, J. P., Dow, R. L., Changelian, P. S., Brissette, W. H., Weringer, E. J., Pollok, B. A. and Connelly, P. A. (1996). Discovery of a novel, potent, and Src family-selective tyrosine kinase inhibitor: study of Lck- and FynT-dependent T cell activation. *J. Biol. Chem.* **271**, 695-701.

Haynes, E. M., Asokan, S. B., King, S. J., Johnson, H. E., Haugh, J. M. and Bear, J. E. (2015). GMFbeta controls branched actin content and lamellipodial retraction in fibroblasts. *J. Cell Biol.* **209**, 803-812.

Hynes, R. O. (2002). Integrins: bidirectional, allosteric signaling machines. *Cell* **110**, 673-687.

Johnson, H. E., King, S. J., Asokan, S. B., Rotty, J. D., Bear, J. E. and Haugh, J. M. (2015). F-actin bundles direct the initiation and orientation of lamellipodia through adhesion-based signaling. *J. Cell Biol.* **208**, 443-455.

King, S. J., Worth, D. C., Scales, T. M. E., Monypenny, J., Jones, G. E. and Parsons, M. (2011). beta1 integrins regulate fibroblast chemotaxis through control of N-WASP stability. *EMBO J.* **30**, 1705-1718.

Klinghoffer, R. A., Sachsenmaier, C., Cooper, J. A. and Soriano, P. (1999). Src family kinases are required for integrin but not PDGFR signal transduction. *EMBO J.* **18**, 2459-2471.

Kobayashi, K., Kuroda, S., Fukata, M., Nakamura, T., Nagase, T., Nomura, N., Matsuura, Y., Yoshida-Kubomura, N., Iwamatsu, A. and Kaibuchi, K. (1998). p140Sra-1 (Specifically Rac1-associated Protein) is a novel specific target for Rac1 small GTPase. *J. Biol. Chem.* **273**, 291-295.

Kostourou, V. and Papalazarou, V. (2014). Non-collagenous ECM proteins in blood vessel morphogenesis and cancer. *Biochim. Biophys. Acta* **1840**, 2403-2413.

Krauthammer, M., Kong, Y., Ha, B. H., Evans, P., Bacchiocchi, A., McCusker, J. P., Cheng, E., Davis, M. J., Goh, G., Choi, M. et al. (2012). Exome sequencing identifies recurrent somatic RAC1 mutations in melanoma. *Nat. Genet.* **44**, 1006-1014.

Kuo, J.-C., Han, X., Hsiao, C.-T., Yates, J. R., III and Waterman, C. M. (2011). Analysis of the myosin-II-responsive focal adhesion proteome reveals a role for beta-Pix in negative regulation of focal adhesion maturation. *Nat. Cell Biol.* **13**, 383-393.

Kutys, M. L. and Yamada, K. M. (2014). An extracellular-matrix-specific GEF-GAP interaction regulates Rho GTPase crosstalk for 3D collagen migration. *Nat. Cell Biol.* **16**, 909-917.

Lawson, C. D. and Burridge, K. (2014). The on-off relationship of Rho and Rac during integrin-mediated adhesion and cell migration. *Small GTPases* **5**, e27958.

Mar, V. J., Wong, S. Q., Logan, A., Nguyen, T., Cebon, J., Kelly, J. W., Wolfe, R., Dobrovic, A., Mclean, C. and Mcarthur, G. A. (2014). Clinical and pathological associations of the activating RAC1 P29S mutation in primary cutaneous melanoma. *Pigment Cell Melanoma Res.* **27**, 1117-1125.

Mitra, S. K. and Schlaepfer, D. D. (2006). Integrin-regulated FAK-Src signaling in normal and cancer cells. *Curr. Opin. Cell Biol.* **18**, 516-523.

Monypenny, J., Zicha, D., Higashida, C., Oceguera-Yanez, F., Narumiya, S. and Watanabe, N. (2009). Cdc42 and Rac family GTPases regulate mode and speed but not direction of primary fibroblast migration during platelet-derived growth factor-dependent chemotaxis. *Mol. Cell. Biol.* **29**, 2730-2747.

Nassar, N., Cancelas, J., Zheng, J., Williams, D. A. and Zheng, Y. (2006). Structure-function based design of small molecule inhibitors targeting Rho family GTPases. *Curr. Top. Med. Chem.* **6**, 1109-1116.

Parsons, M., Messent, A. J., Humphries, J. D., Deakin, N. O. and Humphries, M. J. (2008). Quantification of integrin receptor agonism by fluorescence lifetime imaging. *J. Cell Sci.* **121**, 265-271.

Pollard, T. D. (2007). Regulation of actin filament assembly by Arp2/3 complex and formins. *Annu. Rev. Biophys. Biomol. Struct.* **36**, 451-477.

Ridley, A. J., Schwartz, M. A., Burridge, K., Firtel, R. A., Ginsberg, M. H., Borisy, G., Parsons, J. T. and Horwitz, A. R. (2003). Cell migration: integrating signals from front to back. *Science* **302**, 1704-1709.

Rosenberger, G. and Kutsche, K. (2006). AlphaPIX and betaPIX and their role in focal adhesion formation. *Eur. J. Cell Biol.* **85**, 265-274.

Rottner, K., Hall, A. and Small, J. V. (1999). Interplay between Rac and Rho in the control of substrate contact dynamics. *Curr. Biol.* **9**, 640-648.

Rotty, J. D., Wu, C. and Bear, J. E. (2013). New insights into the regulation and cellular functions of the ARP2/3 complex. *Nat. Rev. Mol. Cell Biol.* **14**, 7-12.

Rotty, J. D., Wu, C., Haynes, E. M., Suarez, C., Winkelman, J. D., Johnson, H. E., Haugh, J. M., Kovar, D. R. and Bear, J. E. (2015). Profilin-1 serves as a gatekeeper for actin assembly by Arp2/3-dependent and -independent pathways. *Dev. Cell* **32**, 54-67.

Sawicka, K. M., Seeliger, M., Musaev, T., Macri, L. K. and Clark, R. A. F. (2015). Fibronectin interaction and enhancement of growth factors: importance for wound healing. *Adv. Wound Care* **4**, 469-478.

Schedin, P. and Keely, P. J. (2011). Mammary gland ECM remodeling, stiffness, and mechanosignaling in normal development and tumor progression. *Cold Spring Harb. Perspect. Biol.* **3**, a003228.

Serrels, B., Serrels, A., Brunton, V. G., Holt, M., McLean, G. W., Gray, C. H., Jones, G. E. and Frame, M. C. (2007). Focal adhesion kinase controls actin assembly via a FERM-mediated interaction with the Arp2/3 complex. *Nat. Cell Biol.* **9**, 1046-1056.

Servitja, J.-M., Marinissen, M. J., Sodhi, A., Bustelo, X. R. and Gutkind, J. S. (2003). Rac1 function is required for Src-induced transformation: evidence of a role for Tiam1 and Vav2 in Rac activation by Src. *J. Biol. Chem.* **278**, 34339-34346.

Silva, J. M., Ezhkova, E., Silva, J., Heart, S., Castillo, M., Campos, Y., Castro, V., Bonilla, F., Cordon-Cardo, C., Muthuswamy, S. K. et al. (2009). Cyfip1 is a putative invasion suppressor in epithelial cancers. *Cell* **137**, 1047-1061.

Slack-Davis, J. K., Martin, K. H., Tilghman, R. W., Iwanicki, M., Ung, E. J., Autry, C., Luzzio, M. J., Cooper, B., Kath, J. C., Roberts, W. G. et al. (2007). Cellular characterization of a novel focal adhesion kinase inhibitor. *J. Biol. Chem.* **282**, 14845-14852.

Swaminathan, V., Fischer, R. S. and Waterman, C. M. (2016). The FAK-Arp2/3 interaction promotes leading edge advance and haptosensing by coupling nascent adhesions to lamellipodia actin. *Mol. Biol. Cell* **27**, 1085-1100.

Takawale, A., Sakamuri, S. S. V. P. and Kassiri, Z. (2015). Extracellular matrix communication and turnover in cardiac physiology and pathology. *Compr. Physiol.* **5**, 687-719.

Tang, H., Li, A., Bi, J., Veltman, D. M., Zech, T., Spence, H. J., Yu, X., Timpson, P., Insall, R. H., Frame, M. C. et al. (2013). Loss of Scar/WAVE complex promotes N-WASP- and FAK-dependent invasion. *Curr. Biol.* **23**, 107-117.

Wang, S., Watanabe, T., Matsuzawa, K., Katsumi, A., Kakeno, M., Matsui, T., Ye, F., Sato, K., Murase, K., Sugiyama, I. et al. (2012). Tiam1 interaction with the PAR complex promotes talin-mediated Rac1 activation during polarized cell migration. *J. Cell Biol.* **199**, 331-345.

Webb, D. J., Parsons, J. T. and Horwitz, A. F. (2002). Adhesion assembly, disassembly and turnover in migrating cells – over and over and over again. *Nat. Cell Biol.* **4**, E97-E100.

Weber, M., Hauschild, R., Schwarz, J., Moussion, C., De Vries, I., Legler, D. F., Luther, S. A., Bollenbach, T. and Sixt, M. (2013). Interstitial dendritic cell guidance by haptotactic chemokine gradients. *Science* **339**, 328-332.

Wolf, K. and Friedl, P. (2011). Extracellular matrix determinants of proteolytic and non-proteolytic cell migration. *Trends Cell Biol.* **21**, 736-744.

Worth, D. C., Hodivala-Dilke, K., Robinson, S. D., King, S. J., Morton, P. E., Gertler, F. B., Humphries, M. J. and Parsons, M. (2010). Alpha v beta3 integrin spatially regulates VASP and RIAM to control adhesion dynamics and migration. *J. Cell Biol.* **189**, 369-383.

Wu, C., Asokan, S. B., Berginski, M. E., Haynes, E. M., Sharpless, N. E., Griffith, J. D., Gomez, S. M. and Bear, J. E. (2012). Arp2/3 is critical for lamellipodia and response to extracellular matrix cues but is dispensable for chemotaxis. *Cell* **148**, 973-987.